Compressive sensing for a general SAR imaging model based on Maxwell's equations

Bing Sun[1a], Haicheng Gu[2], Mengqi Hu[2], and Zhijun Qiao[2b]

[1]School of Electronics and Information Engineering, Beihang University, 37 Xueyuan Road, Haidian District,Beijing, 100191, China

[2]Department of Mathematics University of Texas-Pan American, Edinburg 78539, USA

[a]sun8839@gmail.com [b]qiao@utpa.edu

ABSTRACT

A general echo model is derived for the synthetic aperture radar (SAR) imaging with high resolution based on the scalar form of Maxwell's equations. After the consideration of the general echo model in frequency domain, a compressive sensing (CS) matrix is constructed from random partial Fourier matrices for processing the range CS SAR imaging. Simulations validate the orthogonality of the proposed CS matrix and the CS SAR imaging based on the general echo model.

Keywords: compressive sensing, general echo model, Maxwell's equations, synthetic aperture radar (SAR)

1. INTRODUCTION

Synthetic aperture radar (SAR) has been in development for more than 60 years. Many operations, including strip-map, spotlight, scan, and multiple platform borne SAR systems have become more and more popular in recent years. SAR systems have been used in many fields, such as soil moisture, forestry, wetland, and agriculture. Due to the higher resolution of SAR image required, the accuracies of the echo models and imaging algorithms need improvement. Because the echo model is a kind of output, it forms a theoretical basis for all SAR imaging algorithms. From an engineering point of view, the traditional echo model is the time-delayed signal of the transmitted signal. There are lots of approximations for echo model. Let us recall the echo signal model. The SAR echo is one of electromagnetic wave forms, and Maxwell's equations are the basic and accurate tool for electromagnetic wave measurement. Mathematically, the SAR imaging procedure is an inverse problem of the electromagnetic wave. Many mathematical and practical researchers are interested in these types of inverse problems.[1–5]

In recent studies of SAR and inverse synthetic aperture radar (ISAR), the data size trends larger and larger as the need for high resolution images becomes greater and greater. It costs too much and many times the data cannot be downloaded in real time from some space-borne platforms, such as satellites. How to disperse the data size efficiently and decrease the data ratio is a real problem for engineers. The good news is that compressive sensing (CS) theory addresses at least some of these problems.[6] Random sampling theory, the CS sampling, and construction proposed by Donoho et al in 2006[7–9] and Baraniuk in 2007[10] may also help in this endeavor. Many publications in the literature cast the CS into radar imaging,[11–15] where they analyzed the sparse characteristics of SAR signals in different domains. Those are the fundamentals of reconstructing the scenes from the equivalent down-sampling data set. Another application of the CS-SAR imaging is to construct the CS matrix and its optimization.[16] However, most of the past research works are focused on the classical echo model for SAR[17] and ISAR image.[18]

In this paper, our goal is to analyze a general echo model and construct a new CS matrix for the SAR imaging. We use the partial differential Maxwell's equations to derive the electronic field, and then obtain the general echo model in frequency domain and time domain. Based on this general model, considering the sparse characteristic of the scene, we will construct the corresponding orthogonal CS matrix for the SAR imaging.

Our paper is organized as follows. Section 2 derives the general SAR echo model based on Maxwell's equations. In section 3, a new CS matrix is constructed for the CS imaging based on the above general echo model in frequency domain. In Section 4, simulations are given to validate the orthogonality of the CS matrix and the imaging performance. Some comparisons of two CS methods and the evaluation method with indices are also provided. Section 5 concludes the paper.

Compressive Sensing IV, edited by Fauzia Ahmad, Proc. of SPIE Vol. 9484
948402 · © 2015 SPIE · CCC code: 0277-786X/15/$18
doi: 10.1117/12.2177845

2. GENERAL SAR ECHO MODEL

From the scalar form of Maxwell's equations, the incident and scattering fields are analyzed first, and then the general SAR echo model[19] is derived according to the antenna theory.

2.1 Maxwell's equations and field expressions

In this paper, the simplified scalar form of Maxwell's equations is used directly instead of the vector form of Maxwell's equations.[20] That is

$$\left(\nabla^2 - c^{-2}(\mathbf{x})\,\partial_t^2\right)\varepsilon^{tot}(t,\mathbf{x}) = -j(t,\mathbf{x}) \tag{1}$$

where $\mathbf{x}$ is the three-dimensional position vector, $c(\mathbf{x})$ is the local propagation speed of electromagnetic waves and $c(\mathbf{x}) = c_0$ in free space (usually, c_0 is the speed of light), $\varepsilon^{tot}(t,\mathbf{x})$ and $j(t,\mathbf{x})$ is the total scalar field and the current density on the antenna, respectively. $c(\mathbf{x})$ satisfies $c^{-2}(\mathbf{x}) = c_0^{-2} - V(\mathbf{x})$, where $V(\mathbf{x})$ stands for the target reflectivity function, which will be reconstructed from radar echoes. $\varepsilon^{tot}(t,\mathbf{x}) = \varepsilon^{in}(t,\mathbf{x}) + \varepsilon^{sc}(t,\mathbf{x})$, where $\varepsilon^{in}(t,\mathbf{x})$ and $\varepsilon^{sc}(t,\mathbf{x})$ is the incident scalar field and the scattered scalar field, respectively. And $\varepsilon^{in}(t,\mathbf{x})$ satisfies

$$\left(\nabla^2 - c_0^{-2}\partial_t^2\right)\varepsilon^{in}(t,\mathbf{x}) = -j(t,\mathbf{x}). \tag{2}$$

Then the expressions of scattered field and the incident field are as follows.

$$\varepsilon^{sc}(t,\mathbf{x}) = \int\int g(t-\tau,\mathbf{x}-\mathbf{z})\,V(\mathbf{z})\,\partial_\tau^2\varepsilon^{tot}(\tau,\mathbf{x})\,d\tau d\mathbf{z} \tag{3}$$

$$\varepsilon^{in}(t,\mathbf{x}) = -\int\int g(t-\tau,\mathbf{x}-\mathbf{z})\,j(\tau,\mathbf{x})\,d\tau d\mathbf{z} \tag{4}$$

where $g(t,\mathbf{x}) = \frac{\delta(t-|\mathbf{x}|/c_0)}{4\pi|\mathbf{x}|}$, called Green's function,[21] is the fundamental solution of the partial differential equation $\left(\nabla^2 - c_0^{-2}\partial_t^2\right)g(t,\mathbf{x}) = -\delta(t)\,\delta(\mathbf{x})$.

Considering the single scattering approximation in equation (3), the scattered field is reduced to

$$\varepsilon^{sc}(t,\mathbf{x}) \approx \int\int g(t-\tau,\mathbf{x}-\mathbf{z})\,V(\mathbf{z})\,\partial_\tau^2\varepsilon^{in}(\tau,\mathbf{x})\,d\tau d\mathbf{z} \tag{5}$$

For simplicity, the following analysis is complemented in frequency domain ω instead of time domain t.

$$E_B^{sc}(\omega,\mathbf{x}) = -\int G(\omega,\mathbf{x})\,V(\mathbf{z})\,\omega^2 E^{in}(\omega,\mathbf{x})\,d\mathbf{z} \tag{6}$$

$$E^{in}(\omega,\mathbf{x}) = \int G(\omega,\mathbf{x}-\mathbf{y})\,J(\omega,\mathbf{y})\,d\mathbf{y} \tag{7}$$

where $E^{sc}(\omega,\mathbf{x})$ and $E^{in}(\omega,\mathbf{x})$ is the Fourier transform of $\varepsilon^{in}(t,\mathbf{x})$ and $\varepsilon^{in}(t,\mathbf{x})$, respectively, $G(\omega,\mathbf{x}) = \frac{e^{-ik|\mathbf{x}|}}{4\pi|\mathbf{x}|}$ is the frequency expression of Green's function $g(t,\mathbf{x})$, $k = \frac{\omega}{c}$ is the wave number in range direction, $J(\omega,\mathbf{x})$ is the current source in frequency domain. Then, the scattered field with a theoretical point antenna is

$$E_B^{sc}(\omega,\mathbf{x}) = -\int\int G(\omega,\mathbf{x}-\mathbf{z})\,G(\omega,\mathbf{x}-\mathbf{y})\,V(\mathbf{z})\,\omega^2 J(\omega,\mathbf{y})\,d\mathbf{y}d\mathbf{z} \tag{8}$$

2.2 Mathematical Signal Model

2.2.1 Radiation pattern for a SAR antenna

Generally, the transmitting and receiving antenna is composed with many cells. For the sake of simplicity, a planar radar antenna over an aperture $[-a,a]\times[-b,b]$ is analyzed and the current density I is constant, then the radiation scalar $F(k,\mathbf{x})$ can be expressed by

$$\begin{aligned} F(k,\mathbf{x}) &= \int_{-a}^{a}\int_{-b}^{b} e^{ik\hat{\mathbf{x}}\cdot(s_1\hat{e}_1+s_2\hat{e}_2)} I ds_1 ds_2 \\ &= I\,(2a\,\mathrm{sinc}\,(ka\hat{\mathbf{x}}\cdot\hat{e}_2))\,(2b\,\mathrm{sinc}\,(kb\hat{\mathbf{x}}\cdot\hat{e}_1)) \end{aligned} \tag{9}$$

where $\mathrm{sinc}(x) = \frac{sin(x)}{x}$, $\hat{e} = (\hat{e}_1, \hat{e}_2)$ is corresponding to the antenna direction.

Let $p(t)$ the transmitted signal, then the current density on antenna $j(t, \mathbf{x})$ is proportional to $p(t)$ and independent of position. So, $J(\omega, \mathbf{x})$ is proportional to the spectrum of transmitted signal $P(\omega)$. Then

$$\begin{aligned} F(k, \mathbf{x}) &= P(\omega)\left(2a\,\mathrm{sinc}\left(ka\hat{\mathbf{x}}\cdot\hat{e}_2\right)\right)\left(2b\,\mathrm{sinc}\left(kb\hat{\mathbf{x}}\cdot\hat{e}_1\right)\right) \\ &= P(\omega)\, G_a(k, \hat{\mathbf{x}}, \hat{e}) \end{aligned} \tag{10}$$

where $G_a(k, \hat{\mathbf{x}}, \hat{e})$ is just an amplitude function independent of the transmitted signal, with a function of wavenumber k, which varies for a wideband signal even within a short pulse time duration. In fact, this corresponds to the frequency characteristics of antenna, especially under wide bandwidth.

2.2.2 Mathematic model of received echo

Suppose that the center of antenna is located at $\mathbf{x_0}$, the incident field $E^{in}(\omega, \mathbf{x})$ and scattered field $E_B^{sc}(\omega, \mathbf{x})$ are

$$E^{in}(\omega, \mathbf{x}) = \int_{\mathbf{y}\in antenna} \frac{e^{-ik|\mathbf{x}-\mathbf{y}|}}{4\pi|\mathbf{x}-\mathbf{y}|} P(\omega)\, d\mathbf{y} \approx \frac{e^{-ik|\mathbf{x}-\mathbf{x_0}|}}{4\pi|\mathbf{x}-\mathbf{x_0}|} F\left(k, \widehat{\mathbf{x}-\mathbf{x_0}}\right), \tag{11}$$

$$E_B^{sc}(\omega, \mathbf{x}) \approx -\int_{\mathbf{z}\in target} \frac{e^{-ik|\mathbf{x}-\mathbf{z}|}}{4\pi|\mathbf{x}-\mathbf{z}|} V(\mathbf{z})\,\omega^2 \frac{e^{-ik|\mathbf{z}-\mathbf{x_0}|}}{4\pi|\mathbf{z}-\mathbf{x_0}|} F\left(k, \widehat{\mathbf{x}-\mathbf{x_0}}\right) d\mathbf{z}. \tag{12}$$

When a monostatic SAR receives echoes, the stop-go approximation is applied and therefore the received echo is expressed by

$$S_{rec}(\omega) = \int_{\mathbf{y}\in antenna} E_B^{sc}(\omega, \mathbf{y})\, \mathrm{W}(\omega, \mathbf{y})\, d\mathbf{y} \tag{13}$$

where $\mathrm{W}(\omega, \mathbf{y})$ is the weight function of the antenna cell at the position $\mathbf{y}$. Substitute (12) into (13), we have

$$\begin{aligned} D_{rec}(\omega; \mathbf{x}_0) \approx & -\int_{\mathbf{z}\in target} \left[\int_{\mathbf{y}\in antenna} \frac{e^{-ik|\mathbf{y}-\mathbf{z}|}}{4\pi|\mathbf{y}-\mathbf{z}|} W(\omega, \mathbf{y})\, d\mathbf{y}\right] \\ & \frac{V(\mathbf{z})\,\omega^2 e^{-ik|\mathbf{z}-\mathbf{x_0}|}}{4\pi|\mathbf{z}-\mathbf{x_0}|} F\left(k, \widehat{\mathbf{z}-\mathbf{x_0}}\right) d\mathbf{z}. \end{aligned} \tag{14}$$

Considering the far filed condition, $|\mathbf{y}-\mathbf{z}| \approx |\mathbf{z}-\mathbf{x_0}| - \left(\widehat{\mathbf{z}-\mathbf{x_0}}\right)\cdot(\mathbf{y}-\mathbf{x_0})$ and $|\mathbf{y}-\mathbf{z}|^{-1} \approx |\mathbf{z}-\mathbf{x}_0|^{-1}$ are adopted to produce the following form

$$\begin{aligned} D_{rec}(\omega; \mathbf{x}_0) \approx & -\int_{\mathbf{z}\in target} \left[\int_{\mathbf{y}\in antenna} e^{ik\left(\widehat{\mathbf{z}-\mathbf{x_0}}\right)\cdot(\mathbf{y}-\mathbf{x_0})} W(\omega, \mathbf{y})\, d\mathbf{y}\right] \\ & \frac{V(\mathbf{z})\omega^2 e^{-i2k|\mathbf{z}-\mathbf{x_0}|}}{4\pi|\mathbf{z}-\mathbf{x_0}|^2} F\left(k, \widehat{\mathbf{z}-\mathbf{x_0}}\right) d\mathbf{z}. \end{aligned} \tag{15}$$

Putting the unit weight function $W(\omega, \mathbf{y}) = 1$ yields

$$D_{rec}(\omega; \mathbf{x}_0) \approx -\int_{\mathbf{z}\in target} V(\mathbf{z})\omega^2 P(\omega) \frac{e^{-i2k|\mathbf{z}-\mathbf{x_0}|}}{(4\pi|\mathbf{z}-\mathbf{x_0}|)^2} G_a^2\left(k, \widehat{\mathbf{z}-\mathbf{x_0}}, \hat{e}\right) d\mathbf{z}. \tag{16}$$

Until now, we get the general echo model in frequency domain. According to the properties of Fourier transform, the general echo model in time domain can be expressed by

$$d_{rec}(t; \mathbf{x}_0) \approx \int_{\mathbf{z}\in target} V(\mathbf{z}) \frac{\ddot{p}(t - 2|\mathbf{z}-\mathbf{x_0}|/c)}{(4\pi|\mathbf{z}-\mathbf{x_0}|)^2} \otimes g_a\left(t, \widehat{\mathbf{z}-\mathbf{x_0}}, \hat{e}\right) d\mathbf{z} \tag{17}$$

where $\ddot{p}(t)$ is the second derivative of $p(t)$, $g_a\left(t, \widehat{\mathbf{z}-\mathbf{x_0}}, \hat{e}\right)$ is the inverse Fourier transform of $G_a^2\left(k, \widehat{\mathbf{z}-\mathbf{x_0}}, \hat{e}\right)$, and $\otimes$ is convolution on t. If we neglect the antenna's variety with frequency ω or wavenumber k, that's

$G_a(k,\hat{\mathbf{x}},\hat{e}) \approx G_a(k_0,\hat{\mathbf{x}},\hat{e})$, where $k_0 = \frac{\omega_0}{c}$ is the wavenumber corresponding to the carrier-frequency, the above expression can be simplified by

$$d_{rec}(t;\mathbf{x_0}) \approx \int_{\mathbf{z}\in target} V(\mathbf{z}) \frac{\ddot{p}(t-2|\mathbf{z}-\mathbf{x_0}|/c)}{(4\pi|\mathbf{z}-\mathbf{x_0}|)^2} G_a^2\left(k_0, \mathbf{z}\widehat{-\mathbf{x_0}}, \hat{e}\right) d\mathbf{z} \tag{18}$$

Even some approximation about antenna radiation has been made, we can also find the difference between the above model and the transitional echo model, which is as simple as the summing the delayed signal of the transmitted signal. That is, the general echo is not the direct delay of the transmitted signal but the second order differential function of the transmitted signal. Because Doppler phase is much more important in SAR imaging, and the amplitude modulation is not serious for traditional SAR systems. In,[19] the relation and difference between the general echo model and the classical model were minutely analyzed. However, for some high resolution applications, the differences may not be ignored. In this paper, to avoid error as much as possible, we try to find a CS matrix for the general echo model in frequency domain directly.

3. COMPRESSIVE SENSING IMAGING FOR SAR

3.1 Basics of compressive sensing

Because of the potential advantages for SAR imaging, there has been a wealth of research work directed towards CS since 2006. The spirit of CS is the sparse presentation under some basis. Suppose $\Psi \in \mathbf{C}^{N\times N}$ (in fact, the matrix was defined on $\mathbf{R}^{N\times N}$ originally, and could be expanded to the complex matrix) is the orthogonal basis matrix and $\mathbf{s} \in \mathbf{R}^N$ is the coefficients vector, the signal $\mathbf{x} \in \mathbf{R}^N$ can be expressed by

$$\mathbf{x} = \Psi\mathbf{s} \tag{19}$$

where the transform coefficient $\mathbf{s}$ can be calculated by $\mathbf{s} = \Psi^{-1}\mathbf{x}$ mathematically. If there are only $K(\ll N)$ non-zero values (or small absolution) in $\mathbf{s}$, the signal $\mathbf{x}$ is sparse in the corresponding domain, and can be reconstructed by a few random samples with very high probability. Suppose the linear observing process is $\Phi \in \mathbf{R}^{M\times N}$, where $M < N$, the observation data $\mathbf{y} \in \mathbf{R}^M$ is

$$\mathbf{y} = \Phi\mathbf{x} = \Phi\Psi\mathbf{s} = \Theta\mathbf{s} \tag{20}$$

where the observing matrix $\Theta = \Phi\Psi \in \mathbf{C}^{M\times N}$. Based on CS theory, the reconstruction of the sparse coefficient $\mathbf{s}$ can be resolved by the following optimization problem.

$$\hat{\mathbf{s}} = arg\ min \parallel \mathbf{s} \parallel_0 \ \ s.t.\ \mathbf{y} = \Theta\mathbf{s} \tag{21}$$

Because l_0 normalization optimization problem is difficult to resolve, l_0 normalization is replaced by l_1 normalization for the actual solution. Then the signal $\mathbf{x}$ to be estimated by $\hat{\mathbf{x}} = \Psi\hat{\mathbf{s}}$.

3.2 Compressive Sensing Matrix for SAR Imaging

To apply CS to SAR imaging, we should consider two conditions: the sparsity of signal and the CS matrix. For the first condition, according to the theory of electromagnetic scattering, some target can be thought as combination of several strong scatters; even for some continuous distributed scenes, the sparse coefficients can be found in the frequency domain or wavelet domain, etc. So most literatures have discussed the CS processing for SAR echoes. For the other condition, the previous literatures[22,23] presented one kind of sensing matrices as follows.

$$\Psi = \begin{bmatrix} chirp\left(\frac{N_\tau}{2}\right) & chirp\left(\frac{N_\tau}{2}-1\right) & chirp\left(\frac{N_\tau}{2}-2\right) & \dots & 0 \\ chirp\left(\frac{N_\tau}{2}+1\right) & chirp\left(\frac{N_\tau}{2}\right) & chirp\left(\frac{N_\tau}{2}-1\right) & \dots & 0 \\ chirp\left(\frac{N_\tau}{2}+2\right) & chirp\left(\frac{N_\tau}{2}+1\right) & chirp\left(\frac{N_\tau}{2}\right) & \dots & 0 \\ \vdots & \vdots & \vdots & \ddots & \vdots \\ 0 & 0 & 0 & \dots & chirp\left(\frac{N_\tau}{2}\right) \end{bmatrix} \tag{22}$$

where $chirp\,(i) = rect(\frac{2i-N_\tau}{2N_\tau})exp\{j\pi b\left(\frac{i-0.5*N_\tau}{Fs}\right)^2\}$ is the transmitted linear frequency modulation (LFM) chirp signal, b is the frequency modulation ratio of the chirp signal, f_s is the sampling frequency, τ and $N_\tau = \tau f_s$ is the pulse width and points numbers of the chirp signal, respectively.

This CS matrix is based on the idea that the echo signal is the delay of the transmitted signal, and its orthogonality also was validated. However, according to section 2 of this paper, we have found the general echo model is the expansion of the simple delay model of the transmitted signal, and it is more accurate for some high resolution applications. Our goal is to find a CS matrix corresponding to the general echo model directly.

In the beginning, the received signal after discrete processing from the frequency domain expression (16) can be expressed as

$$D_{rec}(m,n;\mathbf{x_0}) = -\sum_{n=1}^{N_p}\sigma_n\omega_m^2 P(\omega_m)\frac{e^{-i4\omega_m R_n/c}}{(4\pi R_n)^2}G_a^2(\frac{\omega_m}{c},\widehat{\mathbf{z_n}-\mathbf{x_0}},\hat{e}) \tag{23}$$

where the subscript m represents the frequency number for fast time of echo, n represents the target index, N_p the number of the discrete targets, R_n is the range between the n-th target point located at $\mathbf{z}_n$ and the center of the antenna located at $\mathbf{x}_0$, $\omega_m = 2\pi f_s(m/N - 1/2)$ is the discrete frequency, $m = 0, 1, \ldots, N-1$, and N is the number of Fourier transform. Suppose the scatter coefficients vector $\mathbf{\Sigma} = [\sigma_1, \sigma_2, \ldots, \sigma_{N_p}]^T$, the (m,n)-th element of the CS matrix Ψ can be constructed as

$$\Psi_{mn} = \omega_m^2 P(\omega_m)\frac{e^{-i4\omega_m R_n/c}}{(4\pi R_n)^2}G_a^2(\frac{\omega_m}{c},\widehat{\mathbf{z_n}-\mathbf{x_0}},\hat{e}) \tag{24}$$

With these definitions, it is not hard to validate $\mathbf{D_{rec}}(\mathbf{x_0}) = \Psi\mathbf{\Sigma}$. Because we use the general echo model in frequency domain, the CS matrix Ψ is also the function of the general transmitted signal in frequency domain $P(\omega_m)$. For instance, if the transmitted signal is a chirp signal, according to the principle of stationary phase, we can get $P(\omega_m) = Ae^{-i(\frac{\omega_n^2}{4\pi b}+\frac{\pi}{4})}$, where A is a complex constant, and then the CS matrix Ψ becomes

$$\Psi_{mn} = \frac{A\omega_m^2 e^{-i\frac{\pi}{4}}}{(4\pi R_n)^2}e^{-i(\frac{4\omega_m R_n}{c}+\frac{\omega_n^2}{4\pi b})}G_a^2(\frac{\omega_m}{c},\widehat{\mathbf{z_n}-\mathbf{x_0}},\hat{e}) \tag{25}$$

To validate the orthogonality of the CS matrix for different rows, the following correlation will be calculated

$$Cor(\Psi_{m_1 n},\Psi_{m_2 n}) = \sum_{n=1}^{N}\Psi_{m_1 n}\Psi_{m_2 n}^* m_1, m_2 \in [1,N] \tag{26}$$

It is not hard to find that $|Cor(\Psi_{m_1 n},\Psi_{m_1 n})| \gg |Cor(\Psi_{m_1 n},\Psi_{m_2 n})|, (m_1 \neq m_2)$ because of the cophasal stacking effect. And after normalization for each row, the correlation matrix is approximately an identical matrix. The orthogonality will be validated in the next section. On the other hand, besides Gaussian and Bernoulli matrices, another very important class of structured random matrices is the random partial Fourier matrix, which is also the object of study in the very first paper on CS.[9] In fact, a random partial Fourier matrix relates the time domain signal and the sparse spectrum items, also it is the first time to construct an orthonormal basis in $\mathbf{C}^{N\times N}$ rather than $\mathbf{R}^{N\times N}$. It has been proved that the Fourier matrix satisfied the restricted isometry property (RIP) and can be applied to CS reconstruction. The proposed matrix defined by (24) or (25) can be thought as one form of the Fourier matrix, and can be applied for CS imaging for the general SAR echo model. Randomly select M rows from Ψ will generate a random partial Fourier Matrix Θ, the range signal reconstruction from the SAR echoes can be accomplished in range frequency domain instead of the traditional match filtering.

In this paper, the orthogonal match pursuit (OMP) algorithm[24] is unitized for the reconstruction of the sparse signal, which corresponds to the discrete scattering coefficients in SAR imaging. The orthogonality of the CS matrix makes sure the maximum probability of reconstruction quickly.

4. SIMULATIONS

In this section, the properties of the CS matrix Ψ are analyzed first, then the CS imaging for a point scene is simulated with both the previous time-domain CS matrix like (22) and the proposed matrix corresponding to the general echo model defined by (24). The comparison of the range reconstruction results after CS and the final imaging results are given.

4.1 Simulation parameters

The main parameters for the below simulations are listed in Table I. To compare with the time-domain CS method, the most common chirp signal is chosen as the transmitted signal. In order to display the affections of wide bandwidth, the frequency of chirp signal ranges from 800MHz to 1200MHz, and the ratio of bandwidth and carrier frequency is up to 40%.

Table 1: Main simulation parameters

parameter	value
height of antenna	5000 m
velocity of antenna	200 m/s
look angle	45 deg
frequency of carrier	1 GHz
bandwidth of chirp signal	400 MHz
sampling frequency	500 MHz
pulse width of chirp signal	1 us
pulse repetition frequency	500 Hz
number of range cells	1024
number of down-sampled range cells	256
synthetic aperture time	5 s

4.2 Results and discussion

4.2.1 Compressive sensing matrix properties

Since there is some complex magnitude term in (25), the accurate proof of the orthogonality based on (26) is difficult.

The diagonal elements of the correlation matrix trend to 1, and others are very small. This correlation matrix is approximate to the identical matrix, so the CS matrix Ψ can be thought as orthogonal matrix.

4.2.2 Imaging results and evaluation

Before analyzing the simulation results, we discuss the evaluation method first. Fourier interpolation is often applied into the evaluation of the traditional range compressed result or SAR image. However, in the previous CS reconstruction, it is acceptable that the range reconstruction result has no sidelobe,[17,25,26] and Fourier interpolation is not suitable to evaluate the result. This Phenomenon might be explained that when K is 1 or a very small number, after reconstruction of compressive sensing, there is at most only 1 non-zero value in each range profile, like a delta function, and any interpolation does not fit during evaluation. According to our simulation during range CS reconstruction, we still set different sparse coefficients K for a single target, and a bigger K will expose the more sidelobes. Fig. 1 illustrates the increasing process of non-zero points corresponding to different K without interpolation.

The bigger K is, the more obvious the sidelobes are. Also Fourier interpolation can be carried out for this construction with some sidelobes. Meanwhile, we set $K = 11$ when we apply the previous CS matrix to the same echoes.

Moreover, we evaluate the imaging results with Fourier interpolation, shown in Fig. 2. The resolutions and peak side-lobe ratios (PSLR) of both slant range and azimuth profiles are listed in Table 2.

According to Fig. 2, the symmetry along with range direction of the result based on our proposed matrix is better than those based on the previous matrix. That is also the main reason of the slant range PSLR

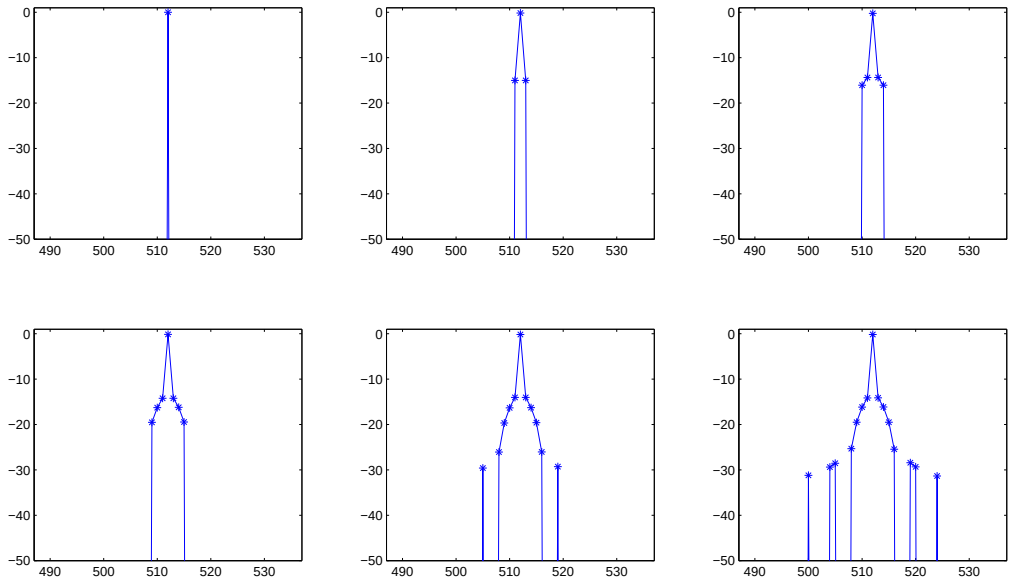

Figure 1: **Non-zero points of reconstruction result corresponding to different K without interpolation.** The six figures correspond to $K = 1, 3, 5, 7, 11, 15$.

difference in Table 2. Also the evaluation indices of our proposed method are much closer to the theoretical indices. Usually the higher the range resolution is, the better the image effect is. However, the more the indices approach the theoretical values, the better the reconstruction algorithm is. In this respect, the CS imaging based on our proposed matrix is much better.

5. CONCLUSIONS

In this paper, a general echo model is derived from Maxwell's equations. The general echo expressions in both frequency domain and time domain are given after generating the scatter filed. The general echo model is the expansion of the classical echo model. Based on the general echo model in frequency domain, a new CS matrix like a random partial Fourier matrix is constructed to apply for the CS imaging. Simulation results validate the orthogonality of the proposed CS matrix and the indices of the CS imaging by our model approach the theoretical values better. Also a bigger sparse number K will expose the sidelobes of the reconstruction, and Fourier interpolation can be applied into evaluating the imaging results.

ACKNOWLEDGMENTS

This work is supported by the National Natural Science Fund of China (Grant No.61301187 and 61328103), and Qiao thanks the U.S. Department of Education GAANN project (P200A120256) for supporting the UTPA mathematics graduate program.

REFERENCES

1. M. Soumekh, M. ; Kaveh, "A theoretical study of model approximation errors in diffraction tomography," *Ultrasonics, Ferroelectrics, and Frequency Control, IEEE Transactions on* **33**(1), pp. 10–20, 1986.
2. M. Soumekh, "A system model and inversion for synthetic aperture radar imaging," *Image Processing, IEEE Transactions on* **1**(1), pp. 64–76, 1992.
3. M. Cheney, "A mathematical tutorial on synthetic aperture radar," *SIAM review* **43**(2), pp. 301–312, 2001.

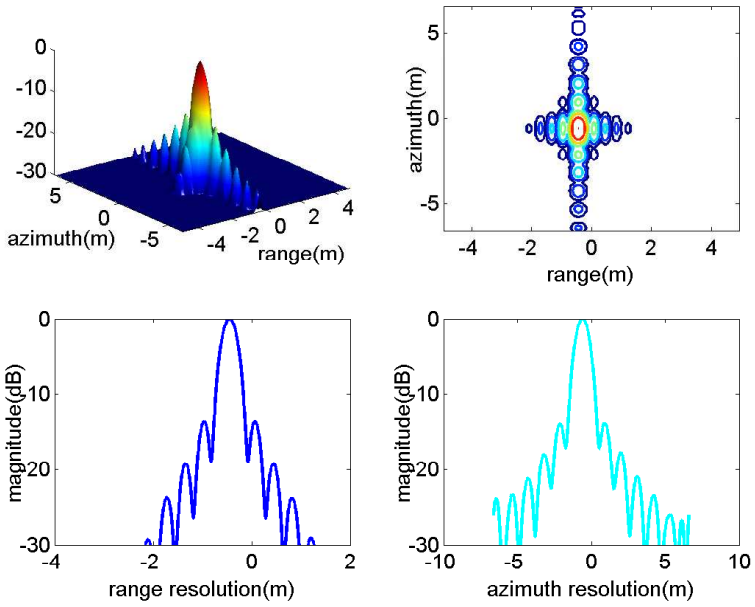

(a)

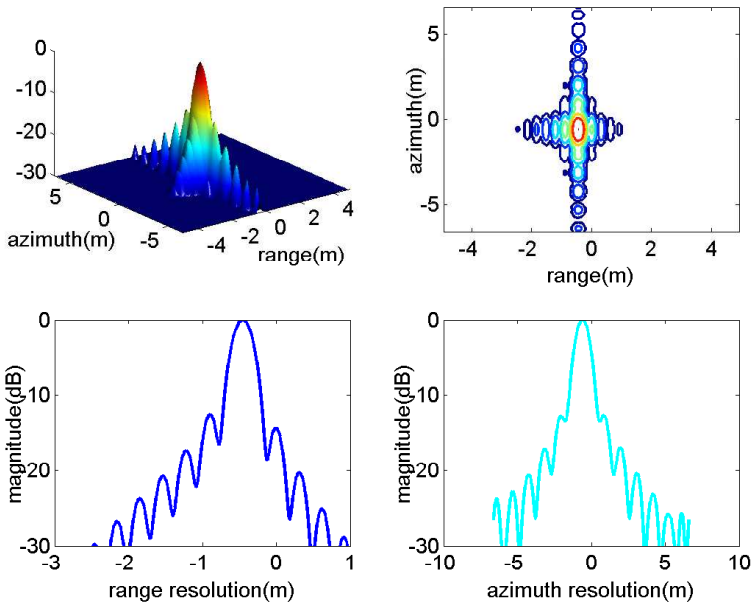

(b)

Figure 2: **Point quality evaluation results.** (a) results based on our proposed matrix in frequency domain; (b) results based on the previous matrix in time domain. The four sub-figures in both (a) and (b) stand the three-dimensional surface, contour image, range profile, and azimuth profile. The two dimensional and one dimensional Fourier interpolations are used, and the times of interpolation are 64 and 1024.

4. C. J. Nolan and M. Cheney, "Synthetic aperture inversion," *Inverse Problems* **18**(1), pp. 221–235, 2002.
5. J. X. Lopez and Z. Qiao, "Filtered back projection inversion of turntable isar data," in *Proc. SPIE*, **8051**, pp. 805109–1–805109–9, 2011.
6. J.-J. Fuchs, "On the application of the global matched filter to doa estimation with uniform circular arrays," *Signal Processing, IEEE Transactions on* **49**(4), pp. 702–709, 2001.
7. E. J. Candès, J. Romberg, and T. Tao, "Robust uncertainty principles: Exact signal reconstruction from highly incomplete frequency information," *Information Theory, IEEE Transactions on* **52**(2), pp. 489–509, 2006.
8. D. L. Donoho, "Compressed sensing," *Information Theory, IEEE Transactions on* **52**(4), pp. 1289–1306, 2006.
9. E. J. Candes and T. Tao, "Near-optimal signal recovery from random projections: Universal encoding strategies?," *Information Theory, IEEE Transactions on* **52**(12), pp. 5406–5425, 2006.
10. R. Baraniuk, "Compressive sensing," *IEEE signal processing magazine* **24**(4), pp. 118–120,124, 2007.
11. R. Baraniuk and P. Steeghs, "Compressive radar imaging," in *Radar Conference, 2007 IEEE*, pp. 128–133, IEEE, 2007.
12. J. H. Ender, "On compressive sensing applied to radar," *Signal Processing* **90**(5), pp. 1402–1414, 2010.
13. L. C. Potter, E. Ertin, J. T. Parker, and M. Cetin, "Sparsity and compressed sensing in radar imaging," *Proceedings of the IEEE* **98**(6), pp. 1006–1020, 2010.
14. E. Lagunas, M. G. Amin, F. Ahmad, and M. Nájar, "Sparsity-based radar imaging of building structures," in *Signal Processing Conference (EUSIPCO), 2012 Proceedings of the 20th European*, pp. 864–868, IEEE, 2012.
15. L. Xu, Q. Liang, X. Cheng, and D. Chen, "Compressive sensing in distributed radar sensor networks using pulse compression waveforms," *EURASIP Journal on Wireless Communications and Networking* **2013**(1), pp. 1–10, 2013.
16. J. Xu, Y. Pi, and Z. Cao, "Optimized projection matrix for compressive sensing," *EURASIP Journal on Advances in Signal Processing* **2010**, p. 43, 2010.
17. Q. Liang, "Compressive sensing for synthetic aperture radar in fast-time and slow-time domains," in *Signals, Systems and Computers (ASILOMAR), 2011 Conference Record of the Forty Fifth Asilomar Conference on*, pp. 1479–1483, Nov 2011.
18. L. Zhang, M. Xing, C.-W. Qiu, J. Li, J. Sheng, Y. Li, and Z. Bao, "Resolution enhancement for inversed synthetic aperture radar imaging under low snr via improved compressive sensing," *Geoscience and Remote Sensing, IEEE Transactions on* **48**, pp. 3824–3838, Oct 2010.
19. B. Sun, Z. Qiao, and J. Chen, "Outer circular synthetic apeture radar imaging based on maxwell's equations," *Journal of Applied Remote Sensing* **6**(1), pp. 063547–1–063547–11, 2012.
20. M. Cheney and B. Borden, *Fundamentals of radar imaging*, vol. 79, Siam, California, 2009.
21. T. Myint-U and L. Debnath, *Linear partial differential equations for scientists and engineers*, Springer, Birkhäuser Boston, 2007.
22. M. Tello Alonso, P. López-Dekker, and J. J. Mallorquí, "A novel strategy for radar imaging based on compressive sensing," *Geoscience and Remote Sensing, IEEE Transactions on* **48**(12), pp. 4285–4295, 2010.
23. P. Xiao, Z. Yu, and C. Li, "Compressive sensing sar range compression with chirp scaling principle," *Science China Information Sciences* **55**(10), pp. 2292–2300, 2012.
24. J. A. Tropp and A. C. Gilbert, "Signal recovery from random measurements via orthogonal matching pursuit," *Information Theory, IEEE Transactions on* **53**(12), pp. 4655–4666, 2007.
25. J. Xu and Y. Pi, "Compressive sensing in radar high resolution range imaging," *Journal of Computational Information Systems* **3**, pp. 778–785, 2011.
26. J. Yang, J. Thompson, X. Huang, T. Jin, and Z. Zhou, "Segmented reconstruction for compressed sensing sar imaging," *Geoscience and Remote Sensing, IEEE Transactions on* **51**, pp. 4214–4225, July 2013.